A: REMOTE SENSING TUTORIAL

Like *Frequently Asked Questions*, a question is posed, e.g., *A1. What is Remote Sensing?* Then, an answer is given[1] with comments and opinions. For cross referencing, each item is labeled, e.g., *A1*.

In Brief …

These FAQs deal with remote sensing, atmospheric windows, spectral bands, spectral radiant energy terms, Standardized Reflectance Factors (SRFs), SRF Indices (SRFIs), c-factors, n-Space, and transformations from one n-Space to another n-Space.

If interested in a particular topic listed below, please do directly to it.

Sec.	Topic: Unique Topics are **Bold**	Pages
A1.	**Remote Sensing** Defined	p. A2
A2.	Types of **Electromagnetic Radiation** Systems	p. A2
A3.	Why Focus on **Spacecraft-Based** Multispectral Data	p. A3
A4.	**Basic Elements** of Remote Sensing & Image Interpretation	p. A3
A5.	Is a Good Image Good Enough	p. A4
A6.	**Aircraft-Based** Multispectral Imagery	p. A4
A7.	**Multispectral Bands**: **MS Band Codes**	pp. A5-A8
A8.	Why Use **Wavelength**	p. A9
A9.	**Atmospheric Windows**	pp. A9-A10
A10.	What do **Image DNs** Represent	p. A11
A11.	**Spectral Radiance** (**SR**) Introduced	p. A12
A12.	**Solid Angle** (**SA**) Defined	pp. A12-A13
A13.	**Spectral Radiance** (**SR**) Defined	pp. A13-A14
A14.	**Spectral Exitance** (**SE**) Defined	pp. A15-A17
A15.	**Spectral Irradiance** (**SI**) Defined	pp. A18-A19
A16.	**Reflectance Factor** (**RF**) and **Standardized Reflectance Factor** (**SRF**) Defined	pp. A20-A22
A17.	Relationship between **SRFsfc** and **SRFtoa**	pp. A23-A24
A18.	**c-Factor** Defined	pp. A24-A26
A19.	**n-Space** Defined	pp. A26-A37
A20.	**n-Space** & **TR Transformation**	pp. A37-A39
A21.	**NDVI & SAVI** & **TR Transformations**	p. A40
	REFERENCES	pp. A41-A42

[1] Jack F. Paris, Ph.D., 2407 Maplewood Cir. E., Longmont, Colorado 80503 USA, *jparis37@msn.com* , 303-775-1195

A1. What is Remote Sensing?

Lillesand *et al.* (2004) define remote sensing as "the science and art of obtaining *information* about an *object* … through the *analysis* of data acquired by a device that is not in contact with the object." This includes sensors that measure gravitational, magnetic, or electric forces; sonic devices; and optical and microwave imagers that sense electromagnetic radiation (EMR). *Scripts by Jack™* deal mostly with remotely-sensed EMR data from a variety of multispectral (MS) systems.

A2. What are the Types of EMR Systems?

- Active EMR Systems:
  - Radar (RAdio Detection And Ranging): Synthetic Aperture Radar (SAR) and InterFerometric SAR (IFSAR)
  - LIDAR (LIght Detection And Ranging)
- Passive EMR Systems:
  - Non-imaging radiometers (a.k.a., spectrometers)
  - Optical EMR imagers (some are imaging radiometers):
    - Single-band imagers, e.g., panchromatic (PAN)
    - Shortwave multispectral (MS) imagers: e.g., blue-light (BL), green-light (GL), red-light (RL), near infrared (N), and middle infrared (M) systems.
    - Thermal infrared imagers
    - Hyperspectral imagers

Some Passive EMR Systems cover the whole earth more than once every day, but at very coarse spatial resolution (250-m or worse). Other Passive EMR Systems capture very high-resolution images (as good as 0.61-m) – but not every day or even every month or year. Active EMR Systems on spacecraft today include only single-band, single polarization combinations of SAR systems.

Organized by spatial resolution, Four Basic Types of Passive EMR Systems include:

- High Resolution: e.g., QuickBird, IKONOS & OrbView 3
- Medium Resolution: e.g., SPOT MS & IRS (Indian Remote Sensing Satellite)
- Low Resolution: e.g., Landsat (MSS, TM, ETM+) & Terra ASTER
- Coarse Resolution: e.g., Terra & Aqua MODIS

A3. Why Focus on Spacecraft-Based MS Data?

Using long focal-length optics, spacecraft-based imagers record MS details as small as 2.44 meters (m). Space Imaging's IKONOS and OrbImage's OrbView-3 both collect 1-m PAN and 4-m MS data.

Being closer to the target usually produces images having better spatial details; however, there are three distinct information-extraction advantages to using spacecraft-based MS imagers to collect remotely-sensed data:

1. The inherently high level of radiometric and geometric data quality. Spacecraft-based MS imagers are expensive and, therefore, are well-engineered. They all collect digital numbers (DNs) that are directly related to spectral radiance (SR) at the top of the atmosphere (TOA). High-quality DNs are essential for automatic information extraction processes.
2. The narrowness of their angular field of view. This image-collection geometry greatly simplifies the algorithms that extract quantitative information.
3. The swath width of the collected image.

A4. What are the Basic Elements of Remote Sensing and Image Interpretation?

Lillesand *et al.*, (2004) discuss nine remote-sensing Elements. The author has restated in a modified form, as follows:

1. Know the characteristics of the *source* of radiant energy.
2. Understand the effects of the atmosphere from the source to the surface.
3. Understand how interactions of radiant energy with earth "surface" materials impart information to image data.
4. Understand the effects of the atmosphere from the surface to the sensor.
5. Know the detection and recording characteristics of the remote sensing system and how these affect information.
6. Be able to produce system-corrected remote-sensing products from the collected data; requires a good understanding at *Element 5*.
7. Interpret and analyze the products from Element 6.
8. Generate specific information products that are focused on well-defined user needs. This Element often serves to define the specific needs for quality and content to guide the activities related to *Elements 1* through *7*.
9. *Present information products to end users.*

The quality of extracted information is no better than the weakest *Element*. In other words, a processing "chain" is only as strong as its weakest link.

A5. Is a Good Image Good Enough?

Even the best looking natural color or color infrared images do not show the full extent of the information that can be extracted from a MS image data set.

Making a "good-looking" image does not require highly-analytical operations. But, producing accurate and consistent information always requires highly-analytical and precise, knowledge-based operations.

Many analysts rely exclusively on their brain and their eyes to "see" information in spatial patterns and perceived colors. While manual photo interpretation is an old and respectable art, this approach often leaves significant information behind.

Among all of the *Elements* in *A4*, *Element 6* is most critical. The good news is that high-quality MS data are now commonly available from spacecraft-based imagers (and from some aircraft-based imagers).

> The quality of system-corrected MS products (*Element 6*) must be high to allow the use of quantitative techniques that apply knowledge about *Element 1* through *Element 4* and processing ideas related to *Element 7 through Element 8* – so that information-extraction processes yield *valuable* information products for end users (which is *Element 9*).

A6. Can Information be Extracted from Aircraft-Based MS Data?

Of course, it can. Some useful information can always be extracted from aircraft-based MS data; but, it is difficult, if not impossible to extract the same high-level of quantitative information that you get from data collected by a well-designed satellite-based MS system. Aircraft-based hyperspectral imagers and some MS imagers have high levels of data quality; therefore, they are suitable for quantitative information extraction.

In general, several important differences exist between aircraft-based MS imagers and spacecraft-based imager data:

- The look-angle difference has already been noted (*A3*).
- Also, aircraft-based systems sometimes suffer band-to-band misregistration problems due to the close-up viewing geometry. Registration is excellent on spacecraft-based imagery.
- Aircraft-based systems often produce DNs that do not have known relationship to absolute physical radiant-energy quantities. Exceptions are hyperspectral imagers. Spacecraft imagery providers produce DNs that usually have known *and linear* relationships to absolute physical radiant-energy quantities. This is a huge advantage for spectra-based mapping.
- Aircraft-based imagery is often little more than, at best, a pretty picture that has poor radiometric fidelity and may have poor geometric fidelity.

A7. What are the Common Spectral Bands Used by MS Imagers?

Each MS image is associated with a limited spectral range within the EMR spectrum that runs from 300 nanometers[2] (nm) to 15,000 nm.

Current spacecraft-based MS imagers each have 3 to 7 MS bands (for land mapping purposes). Some MS imagers also have a PAN band.

The most common shortwave MS bands are highlighted in **bold blue** in the table below:

Table A7. Generic MS Band Definitions.

MS Band CODE	FULL NAME of each MS Band	WAVELENGTH RANGE Generally Associated with each MS Band
CB	**Coastal-Blue Light**	**400 to 450 nm**
BL	**Blue-Light**	**450 to 500 nm**
GL	**Green-Light**	**500 to 600 nm**
YL	**Yellow-Light**	**650 to 750 nm**
RL	**Red-Light**	**600 to 700 nm**
RE	**Red Edge**	**700 to 800 nm**
NA	**Near Infrared, Band A**	**750 to 900 nm**
NB	**Near Infrared, Band B**	**850 to 1,100 nm**
MA	**Middle Infrared, Band A**	**1.1 to 1.3 μm**
MB	**Middle Infrared, Band B**	**1.5 to 1.7 μm**
MC	**Middle Infrared, Band C**	**2.1 to 2.5 μm**
MD	**Middle Infrared, Band D**	**2.1 to 2.5 μm**
ME	**Middle Infrared, Band E**	**2.1 to 2.5 μm**
MF	**Middle Infrared, Band F**	**2.1 to 2.5 μm**
MG	**Middle Infrared, Band G**	**2.1 to 2.5 μm**
TA	Thermal Infrared, Band A	2.5 to 4.0 μm
TB	Thermal Infrared, Band B	4 to 15 μm

CB and YL bands are included as they will likely be used in future MS systems. In addition to a MC band, Terra ASTER has four more middle infrared bands, MD, ME, MF, and MG, with wavelengths that are close to each other; this part of ASTER is like a hyperspectral imager. In these scripts, the author ignores TA and TB. But, he does deal with the remaining 15 bands: CB, BL, GL, YL, RL, RE, NA, NB, MA, MB, MC, MD, ME, MF, and MG as used in 14 MS systems.

[2] A *nm* is equal to one-billionth of a meter (m), i.e., 1×10^{-9} m. Another popular unit of wavelength is the micrometer (μm), which is equal to one-millionth of a meter, i.e., 1×10^{-6} m.

TA and TB bands involve emission physics, rather than reflectance physics. The author also mostly ignores the PAN band due to its wide bandwidth. In addition, TA, TB, and PAN imagers have very different spatial resolutions than the concurrently-collected shortwave MS imagers.

Ranked according to the number of MS bands, here are the MS systems that these SMLs address (now or in a "work in progress").

- Terra ASTER: 9 shortwave MS bands: GL, RL, NA, MB, MC, MD, ME, MF, and MG. Most of these are "hyperspectral" bands in the middle IR.
- Terra MODIS and Aqua MODIS: 7 shortwave MS bands: BL, GL, RL, NA, MA, MB, and MC (plus 29 more lower-resolution bands designed for atmospheric and ocean sensing). The MODIS band-numbering scheme[3] is 3, 4, 1, 2, 5, 6, and 7. RL and NA have a spatial resolution of 250 m, and BL, GL, MA, MB, and MC have a spatial resolution of 500 m.
- Landsat Thematic Mapper (TM) and Enhanced Thematic Mapper (ETM): 6 shortwave MS bands: BL, GL, RL, NA, MB, and MC. The TM and ETM band numbering scheme[3] is 1, 2, 3, 4, 5, and 7. TM6 and ETM6 are TA bands that have a much lower spatial resolution.
- Landsat Multispectral Scanner (MSS): 4 shortwave MS bands: GL, RL, RE, and NB. The MSS band numbering scheme[3] is 4, 5, 6, and 7. MSS6 is usually considered to be a *near infrared* band. However, MSS6 better fits the RE spec (since its bandpass runs from 700 to 800 nm). MSS6 and MSS7 both are poorly located with respect to atmospheric windows.
- Indian Remote Sensing Satellite (IRS) Linear Imaging Self Scanner (LISS): 4 shortwave MS bands: GL, RL, NA, and MB. The LISS band numbering scheme[3] is 1, 2, 3, and 4. This script does not yet deal with LISS data.
- QuickBird 2, IKONOS 2, and OrbView 3: 4 shortwave MS bands: BL, GL, RL, and NA. In all three of these cases, the band numbering scheme[3] is 1, 2, 3, and 4.
- SPOT 4 & 5: 4 shortwave MS bands: GL, RL, NA, and M2. In both cases, the band numbering scheme[3] is 1, 2, 3, and 4.
- SPOT 1 & 2 have 3 shortwave MS bands: GL, RL, and NA. In both cases, the band numbering scheme[3] is 1, 2, and 3. This script does not deal with SPOT data (of any kind). One reason is the variable gain settings for SPOT.

MS bands that are common to all imagers are: GL, RL, and NA or NB. These allow for the production of a Color Infrared (CIR) picture. RL and NA or RL and NB are required for most Vegetation Indices (VIs). NA and NB play about the same role for land mapping.

[3] The MS system band numbers (used by the providers) are listed here in the same wavelength order, from shortest to longest, as two-letter MS band codes in *Table A7*.

Since confusion exists among the different band numbering schemes, the author uses an unambiguous 2-letter MS band code to designate the MS band being processed by these SMLs. He also states and uses the effective wavelength (wLen) for each MS band in these SMLs.

The locations of atmospheric windows (see *A9*) in the EMR spectrum dictate where MS bands should be placed in order to minimize the effects of transmission losses caused by absorption by atmospheric gases. These locations are set by physics and the composition of the earth's atmosphere.

Engineering limitations, such as minimum bandwidth and signal-to-noise requirements, are important also. These considerations usually determine how many bands will "fit" into each available atmospheric window region.

The precise set of characteristics of each MS band varies significantly from imaging system to imaging system, especially for NA, NB, TA, and TB.

Handling variations among MS band radiant-energy characteristics is important, especially for information-extraction algorithms that involve two or more bands.

The classic situation is when a calibrated Vegetation Index (VI) is being produced. Each kind of VI is meant to be calculated from a set of reflectance factors (RFs), not from uncorrected DNs. When the wavelength associated with a MS band changes from one sensor to another, then the precise meaning of each affected VI may change if care is not taken to account for wavelength-dependent shifts.

Every image-processing software package, including TNTmips, has one or more "VI" buttons, e.g., NDVI (normalized difference VI). But, most users wrongly create a VI raster by inputting uncorrected DNs, rather than calibrated RFs. It is no wonder that the resulting VI does not perform as expected nor have the consistency that is expected. *Scripts by Jack™* leads off with a script called SRFI.sml. It will properly prepare image data so that standard VIs can be properly produced by GRUVI.sml or **TASCAP.sml**.

Examine the spectral characteristics of QuickBird[4] (QB) MS imagery (in *Figure A7*, next page) to see how these compare to the general characteristics presented in *Table A7*. The results of this comparison are typical for all MS systems.

[4] QuickBird 2 is owned and operated by DigitalGlobe, Inc., in Longmont, Colorado. Visit www.digitalglobe.com for further details.

Figure A7. QB's MS Bands and PAN Band Responses.

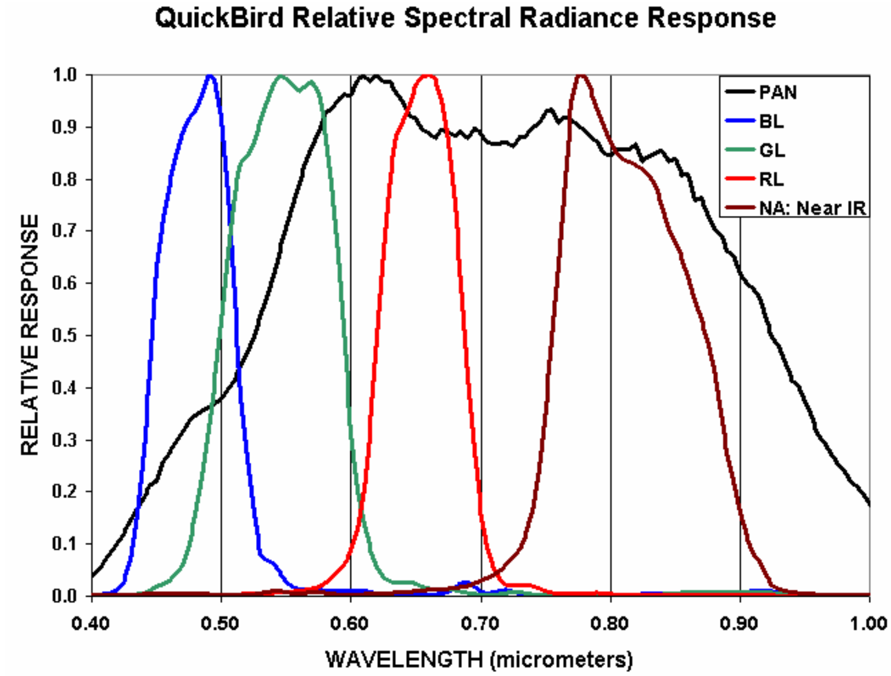

Here are some observations about these bands:

- The **QB BL** band extends significantly into the **generic GL** region.
- The **QB GL** band overlaps significantly with the **QB BL** band.
- A gap occurs between the **QB GL** band and the **QB RL** band.
- The **QB NA** band is not symmetric; it has a peak response on the shorter wavelength end of this band (at 0.78 µm). wLenNA is 0.809 µm.
- The **QB PAN** band has a peak response in the **QB GL-RL gap**.
- These spectral response curves also disagree with some of the information provided by DigitalGlobe, Inc., about **QB MS** bands.

In bold is the stated range of the bandwidths for each QB spectral band. The actual bandwidth range, taken from plots in Figure A7, is given in the parentheses:

- **BL:** **450 to 520 nm** (Plot: 447 to <u>512</u> nm)
- **GL:** **<u>520</u> to 600 nm** (Plot: <u>499</u> to 594 nm)
- **RL:** **<u>630</u> to 690 nm** (Plot: <u>620</u> to 688 nm)
- **NA:** **760 to <u>900</u> nm** (Plot: 755 to <u>874</u> nm)
- **PAN:** **<u>450</u> to <u>900</u> nm** (Plot: <u>526</u> to <u>925</u> nm)

The **bold items** disagree with the "Plot" items, especially for the <u>underlined</u> items. IKONOS has similar spectral properties and discrepancies.

A8. Why is Wavelength Used?

Everyone uses wavelengths to talk about the spectral aspects of remote sensing. So, what's the problem? Wavelength is not a conservative property of radiant-energy. Frequency and photon energy are conservative. So, why is wavelength preferred?

All remote-sensing wavelengths are defined in terms of *what they would be in a vacuum*. *Why is this?* When EMR travels into a denser material medium, the speed of propagation slows down. This causes the actual wavelength to become shorter. Nevertheless, the energy and frequency of the affected photons remains unchanged.

But, we humans relate more easily to a length than to a frequency or to a photon energy amount. An average green-light (GL) photon has a wavelength of about 0.55 μm (in a vacuum). This corresponds to a frequency of 165 teraHertz (1.65 x 10^{14} cycles per second)! 10^{14} cycles per second seems impossibly large. The photon energy is exceedingly small (as measured in Joules, J). So, it is no wonder that we would rather use a wavelength to denote the place that EMR has in a spectrum. In the physics literature, other quantities such as wave number are popular; wave number is directly proportional to frequency, which is directly proportional to photon energy. Wavelength (wLen) is used in these tutorials and in the SMLs.

A9. What are "Atmospheric Windows, and Where are They?"

We all know that clouds and thick haze completely block or strongly attenuate radiant energy across the entire optical EMR spectrum. Clouds and haze become transparent only at microwave wavelengths (e.g., for RADAR, SAR, or IFSAR). Even rain can be transparent to very long microwaves.

When clouds and thick haze are both absent, the "clear" atmosphere still contains gases that significantly absorb certain wavelengths of radiant energy. We don't see these absorption-related wavelengths in the visible region with our eyes.

There are only two kinds of interactions between matter and radiant energy:

- Absorption: This is a process that results in the total conversion of a radiant-energy photon to internal heat energy. This absorbed internal energy will be emitted as radiant energy – but at much longer wavelengths – controlled by the temperature of the absorbing material.
- Scattering: This is a process that results in the redirection of radiant-energy photon with no change in the frequency or energy of the photon.

"Mirror-like" specular reflection is just a special case of scattering. Sometimes, diffuse scattering is also called reflectance. So, a lot of confusion exists about scattering and reflectance in remote sensing.

A stream of radiant-energy photons traveling from the sun to the surface or from the surface to a sensor suffers both absorption and scattering interactions in the atmosphere. Both of these interactions decrease the spectral radiance (SR) of radiant energy in an overall process called attenuation or extinction. SR is discussed in detail in *A13*.

Scattering does not remove radiant energy from the material being considered; it only causes the radiant energy to travel in a new direction.

The primary absorbers in the atmosphere are molecular oxygen, atomic oxygen, ozone, carbon dioxide, and water vapor. These gases absorb radiant energy least efficiently (and thus allow the most efficient transmission) in several, well-known, very specific wavelength ranges called atmospheric windows. A good explanation of atmospheric windows is given by Smith (2001) in the TNTmips tutorial called *Remote Sensing of Environment*. The figure below was adapted from Smith's tutorial.

Figure A9. Atmospheric Windows and Placement of MS Bands

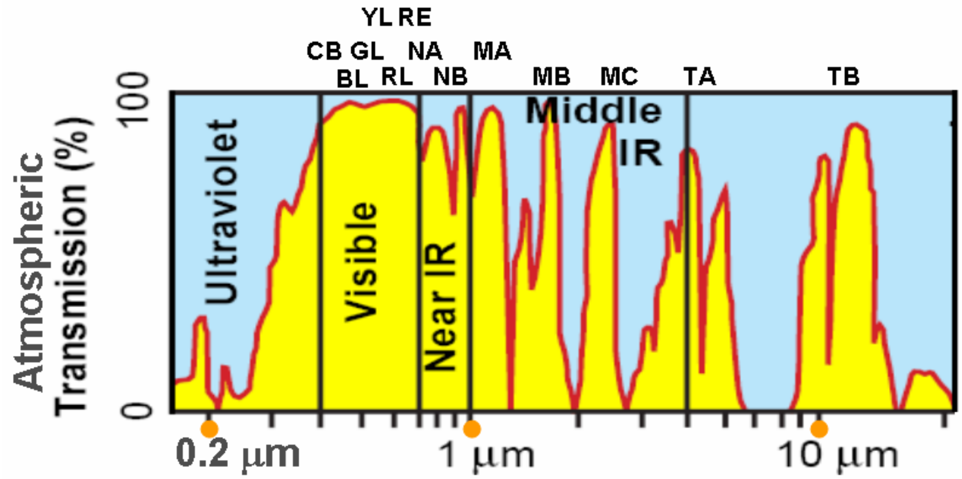

Note that all MS bands are usually placed within one of the atmospheric windows, which are defined as being wavelengths at which the atmospheric transmission is relatively high (the yellow areas in the figure). Also, MD, ME, MF, and MG have about the same wavelengths as for MC above.

The placing of MS bands inside of atmospheric windows makes feasible the use of simple, pragmatic correction factors (called c-factors) for adjusting imagery for atmospheric effects. c-factors are defined and discussed in *A17*.

A10. What do Image DNs Represent?

There are two answers. First, each MS image DN always represents the relative image brightness of each pixel for each designated MS band.

But, for high-quality sensors, each MS image DN also is related *directly* to the average spectral radiance of radiant energy upwelling at the sensor (SRsensor) on a band by band basis. Also, for spacecraft-based imagers, SRsensor is the same as the SR at the top of the atmosphere: SRtoa.

SR has units of radiant-energy power density per unit of solid angle (SA) per unit of bandwidth. Power density, in turn, has units of Watts (W) per square meter (m^2), i.e., W m^{-2}. SA has units of steradians (sr). SA is defined in *A13*. Bandwidth has units of µm. So, the units of SR are W m^{-2} sr^{-1} μm^{-1}. SR will be defined in detail in *A13*.

A general conversion equation, for each MS band, can be written as:

SRsensor[lin,col] = (DN[lin,col] – DNb) * k / ebw (A10a)

- *SRsensor(lin,col)* is the SR at the sensor for each pixel,
- *(lin,col)* denotes the pixel's line and column position,
- *DN(lin,col)* is the relative brightness of the image for each pixel,
- *DNb* is the baseline DN value that corresponds to SRsensor = 0.
- *k* is a conversion coefficient.
- *ebw* is the effective bandwidth of the MS band.

DNb sometimes is equal to zero. For example, this is the case for QB MS data. *k* and *ebw* differ among MS bands. k also differs among gain settings, e.g., for ASTER data.

The quantity, k / ebw, is often combined into a single parameter called spectral k (sk), where

sk = k / ebw (A10b)

With this, *Equation A10a* becomes"

SRsensor[lin,col] = (DN[lin,col] – DNb) * sk (A10c)

Since the units of *k* are W m^{-2} sr^{-1} DN^{-1}, the units of *ebw* are µm, and the units of *SRsensor* are W m^{-2} sr^{-1} μm^{-1}, then the units of sk are W m^{-2} sr^{-1} μm^{-1} DN^{-1}.

There are several other ways to specify how SRsensor is related to DN value.

A11. What is Spectral Radiance (SR)?

Before answering this question, we need understand the concept of solid angle (SA). The answer to *FAQ A11* is therefore deferred to *A13*.

A12. What is Solid Angle (SA)?

Imagine that the sun is being observed in an upward-looking direction from a point just outside of the atmosphere. Ignore the stars and the moon.

A question might be: *How "big" is the sun?* There are several ways to answer this question.

The sun's average radius (**R_S**) is **6.96 x 10^8 meters (m)** (Pasachoff and Kutner, 1978). Thus, the sun's cross-sectional area (**A_S**) is **1.522 x 10^{18} m^2**. So, the sun seems to be really big in terms of square meters.

But, the average earth-sun distance (**D_{ES}**) is **1.496 x 10^{11} m** (Pasachoff and Kutner, 1978). This is a large distance (compared to distances on the earth).

From **R_S** and **D_{ES}**, we can calculate the average angular diameter of the sun, **Θ_{SUN}**, as follows:

$$\Theta_{SUN} = 2 \arctan (R_S / D_{ES}) = 0.533 \text{ degrees} \qquad \textbf{(A12a)}$$

In terms of the average angular size, the sun appears to be small (compared to 360 degrees).

For remote sensing modeling purposes, it is a good thing that the sun occupies only a small part of the total "sky" (i.e., upper hemisphere).

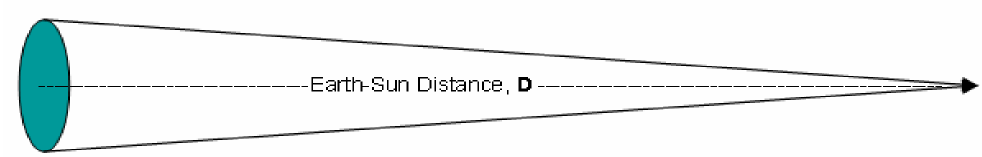

Now, construct a long, skinny cone (as shown above) that extends from your position (on the right) to the sun (on the left). The defined cone contains all of the possible lines of sight from the sun to your vantage point. This cone represents a *physical quantity* called solid angle (SA). In scientific literature, SA is often represented by a Greek symbol, e.g., $\Delta\Omega$. Here, SA is used.

The definition of SA (SAsun, in this case of the sun) is:

$$\text{SAsun} = A_S / D_{ES}^2 = 6.8 \times 10^{-5} \text{ steradians (sr)} \qquad \textbf{(A12b)}$$

The "solid" part of SA name comes from the fact that a SA cone is a volumetric (3-D) object. Plane trigonometry angles occur in 2-D planes. So, "solid angle" is an appropriate name for a 3-D geometric object like a cone. But SA does not have to be defined by a 3-D cone. In general, SA is defined in terms of a projected area at a distance being divided by the square of that distance (no matter how far away the area is from the observer). This definition for SA allows for the easy calculation of the solid angle of a sphere or of a hemisphere, such as the "dome" of the sky or the "sphere" of the universe.

SAsun is a small number (**6.8×10^{-5}** sr). But, is it small relative to another object? Another way to gauge the size of the sun is to compare SAsun to the SA of the whole hemispheric (hemis) sky (SAhemis).

A sphere, with a radius, **r** (m), has surface area of **$4 \pi r^2$**. The SA of a sphere is the sphere's surface area divided by **r^2**. So, SAsphere is **= 4π sr**, which is **12.566 sr**. Half of a sphere is … a hemisphere, e.g., the hemispherical "dome" of the sky. A hemisphere therefore has a SA value equal to half of the value of SAsphere; thus, SAhemis **= 2π sr = 6.283 sr**.

If we do the math, we will find out that SAsun is only **0.0011 %** of the size of SAhemis. So, the sun is very small indeed – so small that the sun acts like a point source of EMR. This makes it easy to estimate the spectral irradiance (SI) of the sun at TOA. SI is discussed in *A15*.

A13. Again, What is Spectral Radiance (SR)?

Suppose that you point a quantitative, calibrated radiometer directly toward the sun from a point near the earth, but above TOA. It will receive a definite (and almost constant over time) amount of radiant energy, **ΔQ**, measured in Joules (J), during a finite increment of time, **Δt**, measured in seconds (sec). If the *perpendicular* receiving area of the radiometer is **ΔA** (in m^2), then, the power density, in $W\ m^{-2}$, is **ΔQ / (Δt ΔA).**

At the *average* earth-sun distance, the power density of the direct sun is **$135.3\ W\ m^{-2}$**. This value is called the solar constant (Weast, 1985). However, its value does, in fact, vary over time with sun-spot cycles and perhaps other long-term trends. This variation in the power density of the direct sun is something like ±1.5%. This uncertainly carries over to each MS band. But, there are other uncertainties that make this source of calibration error less significant for remote sensing purposes.

The power density per unit solid angle (SA) is defined to be the radiance, **L**. That is,

$$L = \Delta Q \,/\, [\Delta t\ \Delta A\ SA] \qquad \textbf{(A13a)}$$

Note that power density part of **L** is measured at the radiometer by the radiometer; but, the SA part of **L** is related to the apparent size of the radiant-energy source (e.g., the sun).

What do you think would happen if you were to move closer to the sun, say to a distance that is one-half of $\mathbf{D_{SE}}$?

Due to the well-known inverse square law of power density, the power density measured by your radiometer would increase by a factor of 4, i.e., $\mathbf{1 / 0.5^2 = 4}$.

But, the SA "size" of the sun would also increase by the same factor of 4! **So, the overall effect on radiance (of your having moved closer to the sun) is nil.** That is, power density per unit solid angle (i.e., the radiance, **L**) does not change as you move from the earth to a different distance between the earth and the sun (or to any other distance). Moving radiant energy through the vacuum of space has no effect on **L**.

This *conservative* nature of radiance is, in fact, the really cool thing about using radiance to keep track of "strength" of radiant energy. Radiance does not change from place to place – *unless* the radiant energy interacts with material objects (like with the atmosphere or with materials on the earth). **Interaction with materials is how a set of remotely-sensed data acquires information about surface materials.**

But, we are not quite finished. We need to define the "spectral" part of spectral radiance. MS imagers, as we have seen, use radiant-energy detectors that have a limited bandpass regarding their wavelength responses. But, radiance is carried by all of the possible wavelengths in the EMR spectrum. It is obvious that the radiance within a narrow MS bandwidth is less than the total radiance carried by all wavelengths. The effective bandwidth, $\Delta\lambda$, is measured in μm. Sometimes, in these SMLs, ebw is used for effective bandwidth.

So, each band's radiance is proportional to its ebw. Thus, if we divide the radiance by ebw, we get the quantity called spectral radiance (SR). SR has units of $W\ m^{-2}\ sr^{-1}\ \mu m^{-1}$. SR is the power density per unit solid angle per unit bandwidth. In physics textbooks, spectral radiance is symbolized by $\mathbf{L}_\lambda$. But, in these SMLs, SR is used for this very useful radiant-energy property.

About SML names: Don't use a name like "Llamda" in SML code. It has an ambiguous character, i.e., the letter "el", (**l**). This looks like the character for the number *one* (**1**). This is especially true when **`"Courier New"`** font is used in SML script. **`Compare l to 1.`** It's really hard to see the difference. It is difficult enough to write SML scripts without having look-alike characters.

A14. What is Spectral Exitance (SE)?

Lillesand *et al.* (2005) (and many other radiant-energy textbooks) define two kinds of hemispherical radiant-energy spectral power density quantities:

- Spectral exitance (SE) is the radiant-energy quantity that relates to the upwelling spectral power density.
- Spectral irradiance (SI) is the radiant-energy quantity that relates to the downwelling spectral power density.

As we will learn later, the reflectance factor, RF, is defined as SE divided by SI, i.e., RF = SE / SI. Thus, RF is a spectral-power-density reflectance concept. Some authorities refer to RF as being the hemispherical-hemispherical reflectance (the upwelling hemisphere's spectral power density divided by the downwelling hemisphere's spectral power density). In the field, RF can be estimated by dividing the SR from a real object by the SR from a non-absorbing, diffusely-scattering reference "white" calibration panel. Both objects have to be irradiated by the same SI (same magnitude and same distribution of incoming SR). And, the "white" calibration panel has to held level.

We will deal further with RF and Standardized Reflectance Factor (SRF) later. But, the field-measured RF is not any more the true value of RF than is the apparent remotely-sensed value of RF. As we will see, a distinction is made between true RF and measurable RF by a quantity that the author calls the Standardized Reflectance Factor (SRF). SRF and its integer indicator, SRFI, is the main focus of the first SML script called SRFI.sml.

Consider *Figure A14* (on page 16).

When radiant energy flows outward (i.e., when it exits or is upwelling) from a reference horizontal surface, then the related spectral power density is called spectral exitance (SE). The units of SE are $W\ m^{-2}\ \mu m^{-1}$. In the SMLs, the author uses SE for spectral exitance.

If the direction of spectral power density flow is inward toward an object, then the related spectral power density is called spectral irradiance (SI).

Figure A14. Solid Angle & Radiant-Energy Terms in Spherical Coordinates.

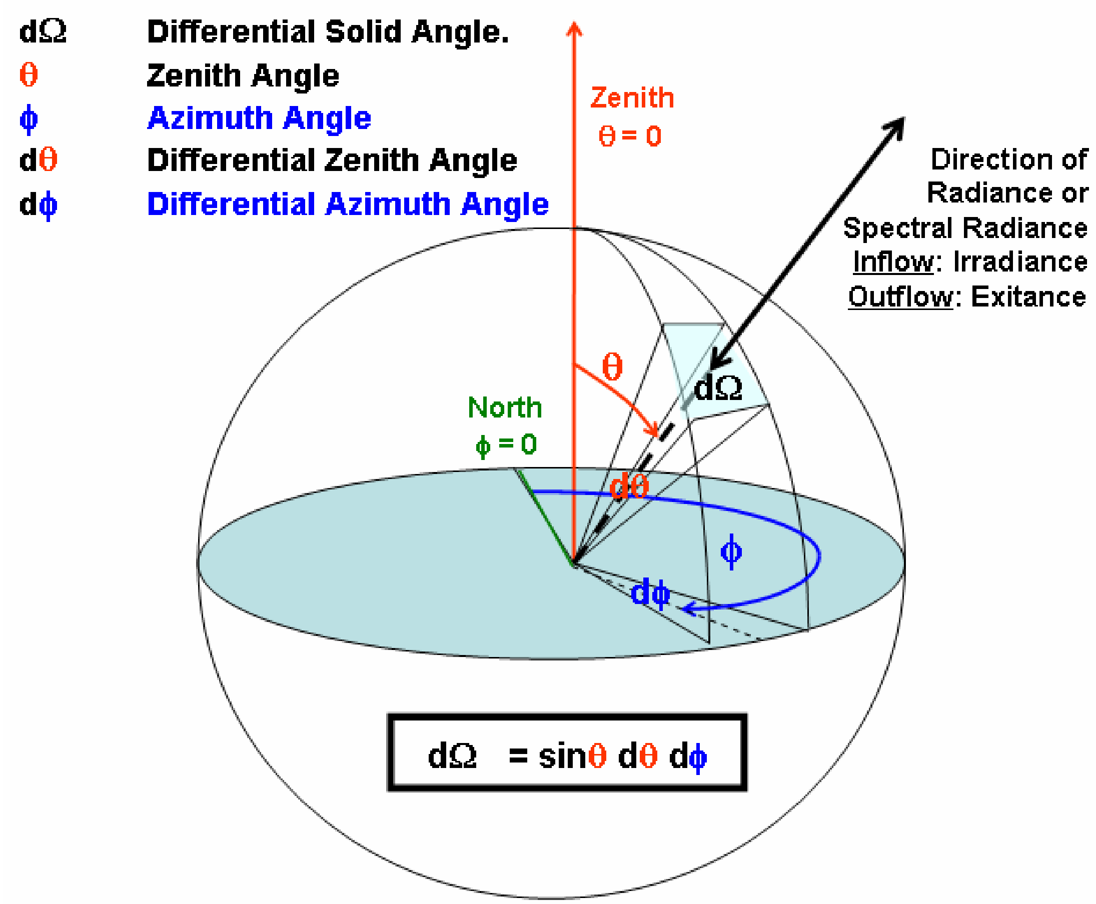

In the spherical coordinate system shown in *Figure A14*, θ is the zenith angle, and φ is the azimuth angle. If the reference sphere has a radius of **r**, then the differential area, **dA**, on the sphere associated with the differential increment of zenith angle, **dθ**, and the differential increment of azimuth angle, **dφ**, is:

$$dA = (r\ d\theta)\ (r\ d\phi\ \sin\theta) = r^2 \sin\theta\ d\theta\ d\phi \qquad \textbf{(A14a)}$$

By the general definition of solid angle, the differential amount of solid angle, **dΩ**, is equal to **dA / r²**. Therefore,

$$d\Omega = \sin\theta\ d\theta\ d\phi \qquad \textbf{(A14b)}$$

SE is an *integrated* quantity that requires the full knowledge of the distribution of spectral radiance (SR) as a function of θ and φ. Mathematically,

$$SE = \int\int SR(\theta,\phi)\ \cos\theta\ \sin\theta\ d\theta\ d\phi \qquad \textbf{(A14c)}$$

SR(θ,ϕ) is the distribution of SR over all upward-looking angles. For this hemisphere, θ ranges from 0 to 90 degrees, and, ϕ ranges from 0 to 360 degrees. The factor, **cosθ**, is present to account for the projected source area. The factors, **sinθ dθ dϕ,** represent the differential solid angle (*Equation A14b*).

A BIG modeling problem in remote sensing is caused by the fact that a MS imager measures SR in only one direction – i.e., the direction related to the single look direction of the imager for each pixel in the image.

The estimation of the true value of SE requires knowing SR**(θ,ϕ)** for all directions over the upper hemisphere. Later in this tutorial, you will see that the true reflectance factor (RF) is defined as SE divided by the spectral irradiance (SI).

Consider the following dilemma: Since the true value of SE cannot be determined from image data alone, then the estimation of the true value of RF is impossible. To make matter worse, it is often difficult to estimate the value of SI accurately. So, there is a double problem associated with the task of getting true estimates of RF.

The usual (pragmatic way) to handle this dilemma is to make a simplifying assumption. But, be wary!

Assumptions can be dangerous! A joke about the word, *assume*, is that it is something that might make an ass out of u and me.

But, we're stuck with an impossible situation! So, the only sensible and pragmatic choice for remote-sensing purposes is to assume that SR has a constant value in all directions, i.e., over all possible values of θ and ϕ angles. *With this assumption*, the relationship between SE and the remotely-sensed value of SR is simple, namely:

$$\mathbf{SE = SR \int\int \cos\theta \sin\theta \, d\theta \, d\phi = SR\ \pi} \qquad \textbf{(A14d)}$$

To not *ever* lose sight of the fact that the true value of SE is unknown, the author defines the value of SE from *Equation (A14d)* as a specific quantity that called the Standardized Spectral Exitance or SSE.

When an image MS DN is converted to SSE and then is converted to the related Standardized Reflectance Factor (SRF), the subsequent analyses of the converted features are more consistent and predictable in this derived frame of reference than in the original uncalibrated, un-standardized DN space.

A15. What is Spectral Irradiance (SI)?

Now, consider the spectral power density of radiant energy flowing inward *from* the upper hemisphere toward a horizontal surface area. Refer to *Figure A14*. This kind of downwelling spectral power density is called the spectral irradiance (SI).

The integral equation for SI is similar to the integral equation for SE, i.e.,

$$\mathbf{SI} = \int\int \mathbf{SR}(\theta,\phi)\cos\theta\,\sin\theta\,d\theta\,d\phi \qquad \textbf{(A15a)}$$

As before, θ ranges from 0 to 90 degrees, and, ϕ ranges from 0 to 360 degrees. As was the case for SE, the trigonometry factors to the right of **SR(θ,ϕ)** represent the projected receiving area and the differential increment of solid angle (see the discussion about SE).

But, in the case of SI, we should not make the simplifying assumption that we made concerning SE. That is, we cannot assume that **SR(θ,ϕ)** as related to SI is constant for all values of the angles, θ and ϕ. *Why not?*

Consider what you would likely see when you look up at the sky during a (cloud-free) sunny morning. You would see a very bright source of SR coming from the sun from essentially a single direction. In addition, you would see a broadly diffuse source of SR coming from everywhere over the rest of the sky. Associated with each of these SR sources is a component (additive) value for SI.

But, back in outer space, above the TOA, only the sun contributes to SI. So, the calculation of SItoa (SI at TOA) is simple:

$$\mathbf{SItoa = SRsun\ \ SAsun\ \ cos\theta_{SUN}} \qquad \textbf{(A15b)}$$

SAsun has a known, nominal value, from Equation A12b, of $\mathbf{6.8 \times 10^{-5}}$ **sr**. This value occurs when the earth-sun distance (esd) is equal to the average earth-sun distance, which is known as 1 Astronomical Unit (A.U.).

Over the course of a year, SAsun changes with the day of the year (DOY) due to the elliptical orbit of the earth around the sun. This change is significant (±3%) and quite predictable by a simple model.

esd is smallest on January 4th and is largest on July 7th. This may surprise you. This would seem to imply that SI is greatest in January and least in July. But, the effect of the solar zenith angle, θ_{SUN}, is much greater than the effects of small changes in esd.

When a MS image is collected on a given date at a given place on the earth and at a given time, the solar zenith angle, θ_{SUN}, is known (related to the solar elevation angle, α_{SUN}) and is reported in the metadata that comes with the imagery.

$$\theta_{SUN} = 90 - \alpha_{SUN} \qquad \textbf{(A15c)}$$

Therefore, SItoa is accurately known for every MS collection date, time, and place. The combination of SRsun and SAsun at the average earth-sun distance is called direct solar spectral irradiance (DSSI), i.e.,

DDSI = SRsun SAsun **(A15d)**

But, returning to our look at the morning sky at the surface of the earth, SIsfc (SI at the surface) is complex. SIsfc can be modeled as the sum of two sources of spectral irradiance: the attenuated spectral irradiance from the sun and the spectral irradiance from the sky (without the sun):

SIsfc = t1 SItoa + SIsky **(A15e)**

SIsky is the part of SIsfc that comes from the all directions distributed over the whole hemispherical sky (but, without the contribution from attenuated SItoa). The factor, **t1**, is the transmittance of the atmosphere along a line from the sun to the surface.

The values of **t1** and **SIsky** are both usually unknown for most remote-sensing situations. However, SItoa is known (from *Equation A15b*). This tutorial deals with these two unknown quantities, **t1** and **SIsky,** later.

If the terrain is not level, then each sloping hillside (and associated aspect) experiences a significantly change in the true value of SI in relationship to **t1 SItoa**. Non-level terrain effects and corrections are handled by a separate SML script called TERCOR.sml (see *FAQs by Jack D.doc*).

If, however, the terrain is level, then we can proceed to the consideration of the effects of surface reflectance factors (RF) – both the true RF and the standardized RF (SRF).

A16. What is Reflectance Factor (RF) and Standardized Reflectance Factor (SRF)?

True reflectance factor (RF) is defined by a simple equation:

RF = SE / SI (A16a)

This definition is based on the Principle of the Conservation of Energy. SI is the spectral power density of radiant energy that is downwelling on a material body. This "body" may be the earth and its atmosphere (as viewed as a single "object" at TOA). Or, this "body" may be a collection of materials at the surface of the earth (as viewed at SFC). Sloping terrain changes the part of SI contributed by attenuated solar irradiance (**t1 SItoa**); terrain slope and aspect do not affect SIsky.

Physically, here is what is taking place. Some fraction of total incoming SI is absorbed by the material object. That fraction is called the absorptance factor (AF), which has a value between 0 and 1. That is, AF is defined as:

AF = [Absorbed Spectral Power Density] / SI (A16b)

If AF = 1, than the "body" is a blackbody and it has no reflectance. AF is a radiant-energy term that you seldom see in discussions about remote sensing. That's too bad, for AF is a great way to understand how interactions between radiant energy and matter imprint information on the remote-sensing signals.

Conservation of Energy requires that the spectral power density *that is not absorbed* must emerge (exit) *from* the material as an upward flowing spectral power density, which is what we call SE. Technically, the absorbed spectral radiant energy also must emerge; but, radiant-energy physics tells us that this happens at the longer wavelengths associated with thermal emission, i.e., in the thermal infrared and thermal microwave.

Therefore,

SE = SI (1 – AF) (A16c)

Materials absorb in a wavelength-selective manner, i.e., the AF varies with wavelength. That is, each kind (and condition) of material has an absorption spectrum. The absorption spectrum is inferred from the observed RF spectrum in a way that is the inverse of the absorption spectrum.

The confusion between AF and RF leads to some rather ridiculous notions in remote-sensing literature. My favorite is the idea that chlorophyll "causes" a high RF in the NA or in the NB. Actually, chlorophyll has no interaction with NA. The absence of absorption by chlorophyll (or any other plant pigments) in the NA or in the NB leads to low AF values, and consequently to high RF values. But, even leaves without chlorophyll have a high NA and NB reflectance. More importantly, chlorophyll strongly absorbs RL and BL and GL (somewhat weaker). The high AF of chlorophyll in the BL, GL, and RL bands is coupled with the low AF in the NA or NB bands to produce a MS RF "signature" for chlorophyll that is unique.

As discussed previously, the **BIG** problem with *Equation A16a* as a definition for RF is that we can never know the true value of SE. We can never know the true value of SE, and we may not know the true value of SI. SI is more predictable for level terrain. But, it still involves an unknown transmittance, **t1**, and an unknown sky spectral irradiance, **SIsky**.

However, we can use Standardized SE (SSE) from *Equation A14d*. SSE was based on a simplifying assumption. We know that this assumption is not strictly true. But, using this assumption gets us past the difficult problem of not being able to estimate SE. When we invoke an assumption like that, we get a technically different reflectance factor – one called the Standardized Reflectance Factor (SRF), i.e.:

SRF = SSE / SI **(A16e)**

Of course, in both cases, RF or SRF, we also need to know the value of **SI**. Knowing SItoa is easy (see *Equation A15b*), i.e.,

SRFtoa = SSEtoa / SItoa **(A16f)**

where **SItoa = DSSI** $\cos\theta_{SUN}$ and SRFtoa is the Standardized Reflectance Factor reference to the top of the atmosphere.

DSSI is fairly well known at TOA. The plots in *Figure A16A* and *Figure A16b* show how DSSI varies with wavelength (wLen) at an earth-sun distance of 1 A.U.

Figure A16A. DSSI as a Function of Wavelength in the Visible Spectrum.

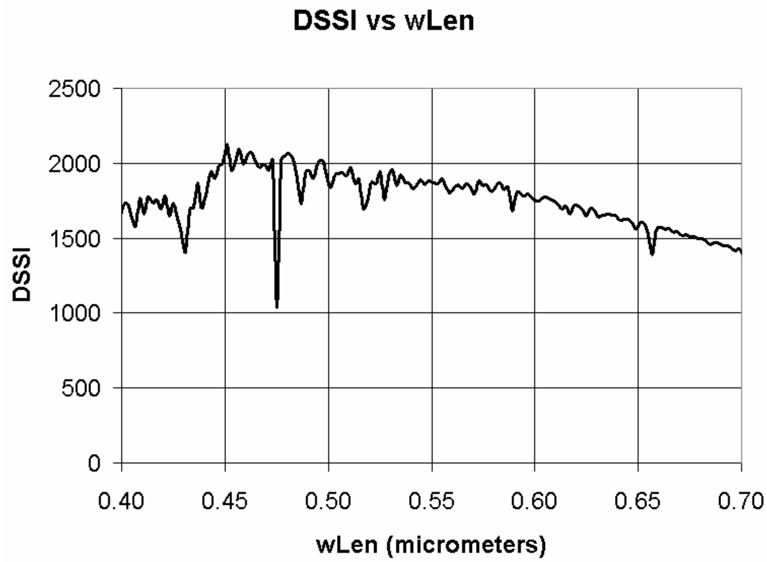

Figure A16B. DSSI as a Function of Wavelength in the Visible, Near Infrared, and Middle Infrared Spectrum.

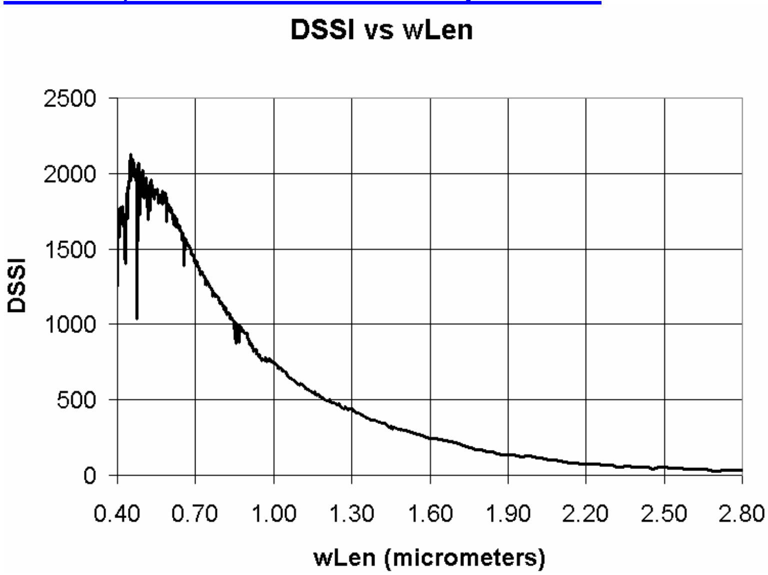

The rapidly-changing aspects of DSSI in *Figure A16A* are caused by low-density gases in the outer fringes of the sun. MS effective bandwidths (ebw) are much broader than these details. In fact, a fixed value for DSSI can be assumed for each MS band of each MS imager.

Figure A16B shows the rapid decrease in DSSI that occurs as wavelengths change from the visible bands (BL, GL, RL, and RE) into the near infrared bands (NA and NB in *Table A7*) and then into the middle infrared bands (MA through MG) as defined in *Table A7*).

A17. So, How does SRFsfc relate to SRFtoa?

This question can be answered by the use of a simple model. This simple model is used in SRFI.sml.

Start with SItoa (spectral irradiance at TOA). SItoa is caused strictly by the sun. Thus, SItoa is a well-known quantity for any spectral band of any MS system. SItoa varies only as a quantitative function of DOY and solar zenith angle, θ_{SUN}. That is, SItoa is given by *Equation A15b*. So, we fully understand the source of radiant energy (*Element 1* in *A4*).

Next, follow SItoa from TOA to SFC. From *Equation A15d*,

SIsfc = t1 SItoa + SIsky (A17a)

This process relates to *Element 2* of *A4*. Unfortunately, we are not likely to know the precise magnitudes of **t1** and **SIsky**. But, let's move on to consider the interactions of **SIsfc** with surface materials. *Equation A16e* gives us a pragmatic way to handle the effects of surface materials through the SRFsfc factor. Applying this to SIsfc from above, we get:

SSEsfc = (t1 SItoa + SIsky) SRFsfc (A17b)

SRFsfc is the standardized RF of materials as would be viewed just above the surface. SSEsfc is the standardized spectral exitance that would be seen just above the surface at the viewing angle used by the MS imager. SRFsfc relates to *Element 3* in *A4*.

SSEsfc has a related spectral radiance called SRsfc. An expression for SRsfc, based on *Equation A14d*, is:

SRsfc = SSEsfc / π (A17c)

But, each MS imager can measure only SRtoa in one direction – the look direction of the imager. Nevertheless, as SRsfc travels upward from the SFC to TOA, the atmosphere attenuates it (by a transmittance factor **t2**). This is the transmittance of the atmospheric path between the surface and the sensor. As is the case for **t1**, the value of **t2** is not precisely known. At TOA, the imager detects this attenuated ray *plus* an additive contribution that comes from reflectances taking place within the atmospheric path itself. This additive component of upwelling SR is called the atmospheric-path's spectral radiance: SRpath. Putting all of these items together, we can write that:

SRtoa = SRpath + t2 SSEsfc / π (A17d)

SRpath and **t2** relate to *Element 4* in *A4*. Therefore, using terms from *Equation A17b*,

SRtoa = SRpath + (t1 SItoa + SIsky) t2 SRFsfc / π (A17e)

There are five unknowns in this equation: SRpath, **t1**, SIsky, **t2**, and **SRFsfc**.

A calibrated MS imager provides a value for **SRtoa** for each DN in each image raster. This fact relates to *Elements 5 & 6* in *A4*. We know the precise value of **SItoa** from a model driven by the DOY and solar elevation angle.

Use *Equations A14d and A16e* to convert SRtoa to SR**F**toa. That is, if we multiply *Equation A17e* by (**π / SItoa)**, we get:

π SRtoa / SItoa = SRFtoa =

= SRFpath + (t1 SItoa + SIsky) t2 SRFsfc / SItoa (A17f)

Define **SRFapc** to be the atmospheric-path-corrected (apc) SRFtoa (seen at TOA). That is,

SRFapc = SRFtoa – SRFpath (A17g)

Therefore,

SRFapc = (t1 SItoa + SIsky) t2 SRFsfc / SItoa (A17h)

Solve *Equation A17h*, for **SRFsfc**. This yields the very useful and simple final set of equations, *Equation (A17i)* and *Equation (A17j)*. That is:

SRFsfc = c SRFapc (A17i)

Where, the aggregate **c-factor** involves three unknowns: **t1**, **t2**, and **SIsky**, and one known parameter, **SItoa**, and where

c = 1 / [t2 (t1 + SIsky / SItoa)] (A17j)

*A18. What are the Values for **c** for Each MS Band?*

When there is no atmospheric attenuation, then **t1** = 1, **t2** = 1, and **SIsky / SItoa** = 0. Thus, the corresponding value for **c** would be **1**.

As the atmosphere becomes more attenuating (thicker), the value of **c** increases to values greater than 1.

For any given atmosphere, **c** increases as the wavelength decreases. Thus, the largest value of **c** will be for the BL band.

In SRFI.sml, a power-law model (based on Chavez, 1996) is used to predict the value for **c** for each MS band wavelength (wLen). This forces **c** to vary with wavelength in systematic and logical ways. Since the RL band is in the middle of the wavelength distribution for MS sensors, an assumed value is assigned to **cRL, equal to 1.34,** as input to the power law model. This script also uses a separate power-law model to adjust estimates of SRFpath for continuity in terms of wavelength. Both **c** and SRFpath depend on how the atmospheric attenuation losses vary with wavelength (wLen). The power laws fit well with actual data when RL is used as the basis for them.

From *Equation A17i*, it is easy to estimate the value of **c** for a given MS band from reliable information about SRFsfc and SRFapc for the same MS band. That is, letting **XX** indicate the MS band being processed:

cXX = SRFsfcXX / SRFapcXX **(A18a)**

By experience with c-factors from data like this, the author has seen that the variation in c from band to band fits well with a general power law equation.

The power-law models for **c** and for **SRFpath** are discussed fully in *FAQs_by_Jack_B.doc*, which provides full information about SRFI.sml.

They both involve separate power factors, pc and p, that each usually have a value between 2 and 3. For cases of relatively low atmospheric attenuation, as is characteristic of MS bands in atmospheric windows, these power factors are consistent with mixed Rayleigh and Mie scattering models that allow the aerosol optical depth to vary systematically with wavelength following a general power law equation.

The general forms of these power-law equations related to c and SRFpath are (all parameter for each MS band, **XX**):

cXX = 1 + (cRL – 1) * (wLenRL / wLenXX)^pc **(A18b)**

and

SRFpathXX = SRFpathRL * (wLenRL / wLenXX)^p **(A18c)**

pc may vary from spectral region to spectral region. As wLenXX become longer and longer, **cXX** approaches 1 and **SRFpathXX** approaches 0. For these models to produce reasonable estimates, the controlling parameters must be accurate: **cRL** and **pc** for **cXX** predictions and **SRFpathRL** and **p** for **SRFpathXX** predictions.

In SRFI.sml, reliable estimates for SRFpathBL and/or SRFpathGL with SRFpathRL are used to find the optimum value for **p**. SRFpath is difficult to measure for RE, NA, NB, MA, MB, and MC through MG. But, these values are also very small in comparison to the values for CB, BL, GL, YL, and RL.

The default value for **cRL** (called icRL) set to **1.34** with a provision for the user to modify this value, if he or she has a valid reason to do so.

The value for **pc** is set equal to **2.27114** (based on the author's experimental finding and *Equation A18A*).

A19. What is n-Space?

Spectral information extraction algorithms treat MS data sets as "points" in an n-dimensional Feature Space called **n-Space**. Remote-sensing output products often involve "locations," "distances," and "angles" in n-Space. When n = 1, 2, or even 3, the concept of n-Space is easy to understand. We can draw diagrams that show how MS data "plots out" on a single axis (1-Space), on a sheet of paper having two axes (2-Space), or within a 3-dimensional volume (3-Space). But, when we start dealing with n > 3, i.e., 4-Space, 5-Space … out to n-Space, visual plots don't work anymore. For example, since Landsat 7 ETM+ has 6 MS bands, each image pixel has 6 DNs – one for each MS band – that, as a set, define a single point in 6 Space. We can answer questions about "locations," "distances," and "angles" in 6-Space by using mathematical equations, such as, the Euclidian distance between two points in 6 Space.

So, the question here is: What is n-Space?

n-Space is *not* a geospatial or map-like space, i.e., one that has geographic locations associated with each location. Rather, it is a feature space involving a set of n features. n-Space can, and often does, have more than 3 coordinates. Each coordinate of n-Space is a number that relates to a particular feature. Each feature in n-Space is considered to be a specific property of the material in each pixel of an image. An n-Space coordinate value might be simply the image brightness DN value from single spectral band image raster, e.g., the DN value from a RL image or the DN value from a NA image. Better yet, a n-Space coordinate value might also be a calibrated reflectance value from a selected image raster, e.g., a Standardized Reflectance Factor Index (SRFI[5]) value in the RL image or in the NA image. Other types of features for n-Space coordinates might be a Vegetation Index (VI), a Tasseled Cap (TC) value, a scene texture indicator, a terrain slope indicator, a terrain aspect-angle indicator, or an environmental variable such as temperature or rainfall. An n-Space component could be the same kind of biophysical variable, but collected on a separate date.

[5] SRFI is a numeric value equal to the SRF value (as a fractional reflectance) times 10,000. For example, a SRFI value of 1000 corresponds to a fractional reflectance factor of 0.1, which is 10% reflectance.

This FAQ also discusses scale-changing and scale-preserving transformations to n-Space. Transformations and conversions are usually required to properly set up a new n-Space for quantitative algorithm applications involve in some kinds of information extraction processes.

Let's start with 1-Space, which is familiar case to anyone who has done univariate analyses of a set of numeric data. Only, it was seldom called by a name like 1-Space.

1-Space: A histogram plot of data related to one MS band image

Consider the DNs in a single image raster. They represent the relative brightness of a scene as this varies from pixel to pixel. In the related 1-Space plot, the location of each DN occupies a "point" on the 1-Space axis:

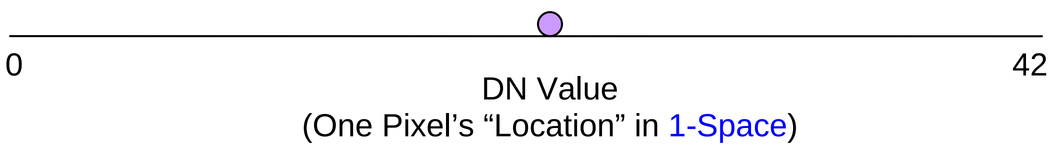

By adding the remaining DN-related "point" locations on the 1-Space axis, you will likely see that the 1-Space points have an uneven density:

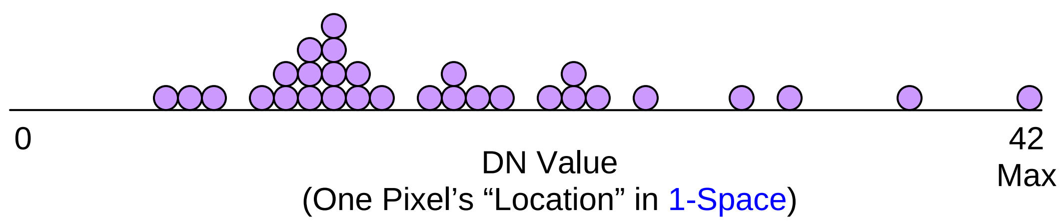

This source raster had only 30 pixels – 30 DN values. A 1-Space plot looks like a standard histogram, which is the common way for an analyst to view the characteristics of a data set in 1-Space. However, another way to show the point density distribution for 1-Space data is to use a **color code**. Assign the following colors to associated point densities: **Black** for **0**; **Gray** for **1**; **Blue** for **2**; **Green** for **3**; and **Red** for 4 (or more). With this color code, the 1-Space plot above looks like this:

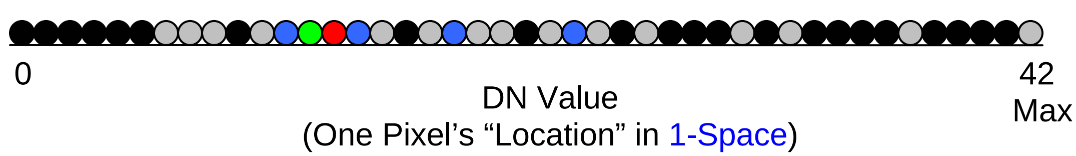

TNTmips has a Raster Histogram tool that shows the point-count density distribution of a set of pixels versus the related DN values. For a whole

QuickBird MS scene (collected over Yuma, CO, on July 2, 2003), the red-light (RL) DNs (called RL) have the following point-count density distribution over the whole range of DN values in the RL raster, which runs from 62 to 2047.

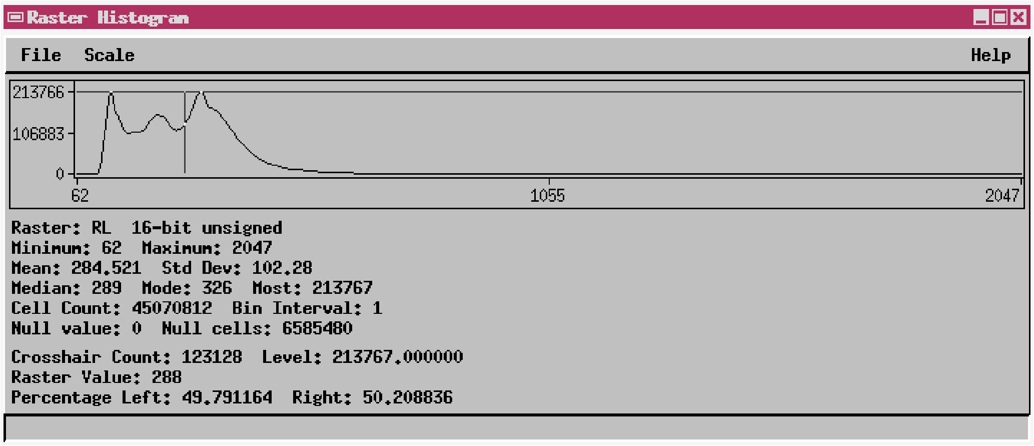

Instead of a "pile" of 1-Space point symbols, the Raster Histogram tool uses a continuous line to indicate the height of the pile for each possible DN value.

Hundreds of thousands of points pile up at some 1-Space RL DN locations.

The Raster Histogram provides several important univariate statistical values:

- Minimum (smallest non-Null DN value)
- Maximum (largest non-Null DN value)
- Mean (average DN value – not counting Null-valued pixels)
- Std Dev (standard deviation of DN values about the Mean – without Nulls)
- Median (DN that is near the 50 percentile cumulative distribution point)
- Mode (DN value for the Most dense location in this 1-Space plot)
- Cell Count (number of non-Null pixels), and
- Null cells (number of Null pixels)

The vertical line marks a single location, Raster Value: 288; 123,128 pixels have a DN value of 288.

The TNTmips Raster Histogram subobject contains a text list of the point density count at every non-zero density location in a designated 1-Space. These data may be imported to a spreadsheet for more detailed analysis. This is a tedious process; but, one that is useful to examine.

For the same Yuma, CO, data above, two sets of 1-Space plots are shown on the next page.

The first set of figures on the following pages (*Figures A19A-A19C*) is for the RL band. Two figures (*Figures A19D-A19E*) are for the NA band.

*Figure A19A. Bar-Chart Plot of **RL** Data as a Histogram-Type 1-Space Plot.*

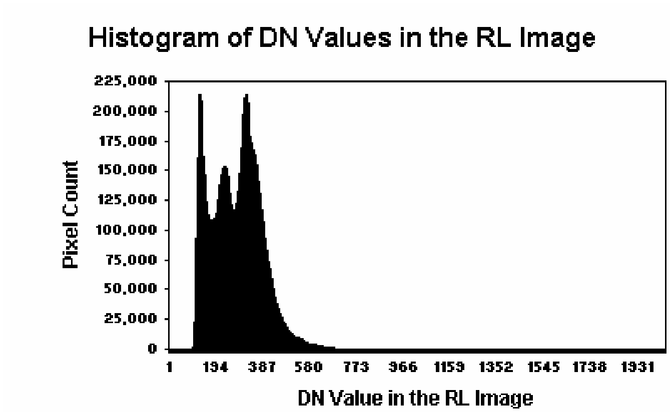

The densest parts of this 1-Space plot are for the lower end of the DN scale.

*Figure A19B. X-Y-Plot of **RL** Data as a Histogram-Type 1-Space Plot.*

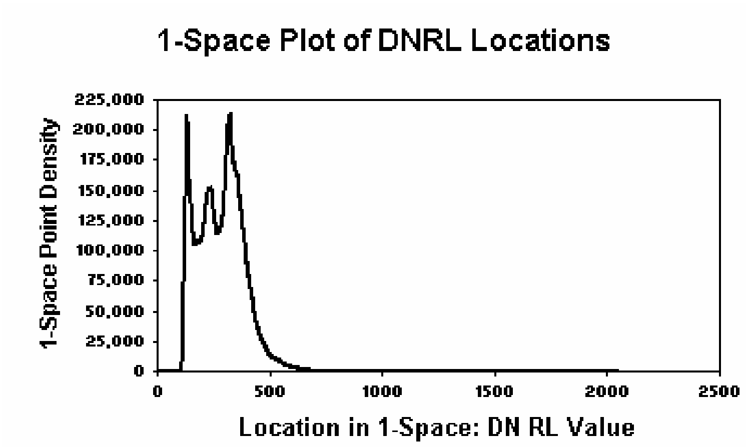

The X-Y Line plot here is more flexible than the Bar-Chart type histogram. It can be easily expanded by changing the range of the X (DN RL) scale.

*Figure A19C. Truncated X-Y Plot of **RL** Data as a Histogram-Type 1-Space Plot (Selected to Focus on the Higher Density Parts of the 1-Space)*

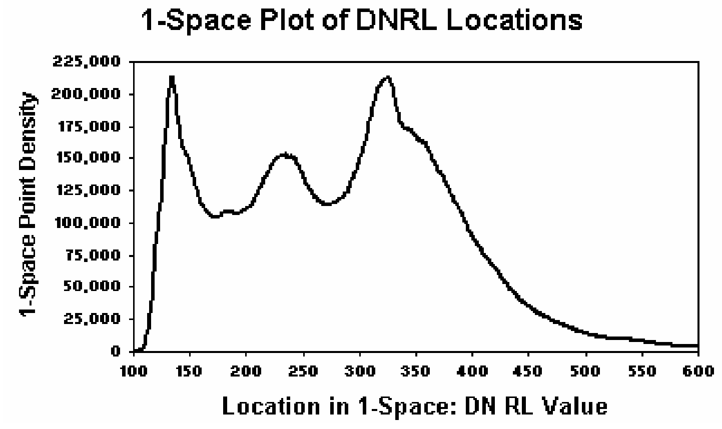

This expanded (truncated scale) plot implies that three kinds of biophysical objects exist in the scene. Dark objects (DNRL < 170), Medium-Bright objects (171 < DNRL < 270), and Bright objects (DNRL > 271). Roughly, these three classes correspond to dense vegetation and water materials, mixed soil and vegetation objects, and non-vegetation objects (roads, rooftops, etc.). But, relying on 1-Space locations (relative to DNRL) for land-cover classification is not optimal. As noted, X-Y Line plots are more flexible than the Bar-Chart type histogram. So, only the latter two types are shown below for the NA band.

Figure A19D. X-Y-Plot of NA Data as a Histogram-Type 1-Space Plot.

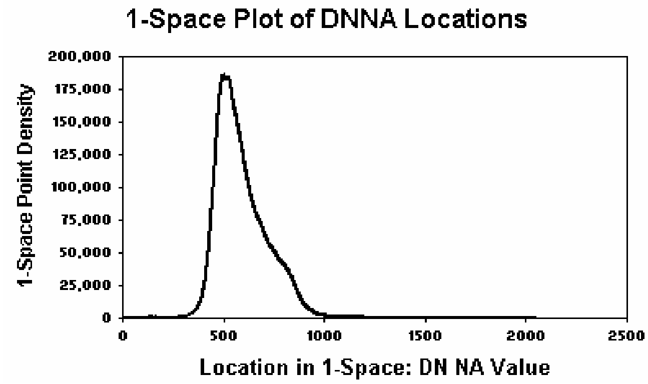

Again, this DNNA 1-Space is most dense for the lowest DN values.

Figure A19E. Truncated X-Y Plot of NA Data as a Histogram-Type 1-Space Plot (Selected to Focus on the Higher Density Parts of the 1-Space)

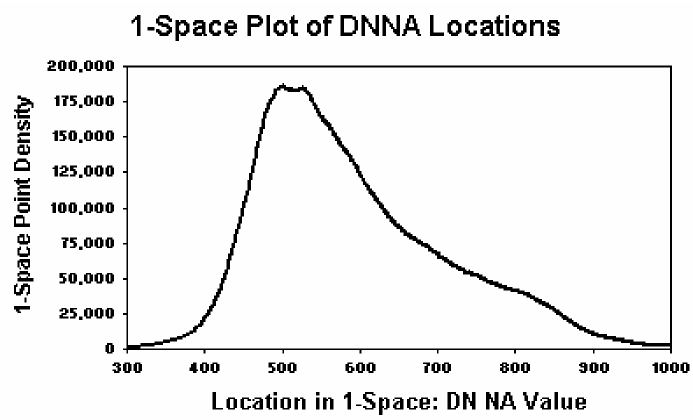

Contrary to the 1-Space associated with DNRL, the DNNA 1-Space has no logical breaks in density. Thus, it alone is not likely to be useful for dividing the scene up into different land-cover classes. However, DNNA is known to be useful, even when used alone, as a reliable indicator of relative biomass density or relative leaf area index for cases where the DN values are in the medium to higher range (say, DNNA > 600) for vegetated pixels.

Fortunately, the confusion that exists within any 1-Space can be better resolved by mapping out the distribution of data densities in a 2-Space, e.g., DNNA vs. DNRL.

2-Space

Consider an example of 2-Space that involves the DN value for RL and the DN value for NA. Plot a point in 2-Space by using two orthogonal axes: X and Y. Let DNRL be the distance of a point along the X-axis; let DNNA be the distance of a point along the Y-axis. DNNA vs. DNRL, shown below, is called a NA vs. RL plot. Suppose a single pixel has a pair of DN values of 10 & 15 for RL and NA, respectively. That point has a location in 2-Space as shown below.

Figure A19F. One point in 2-Space: DNNA vs. DNRL.

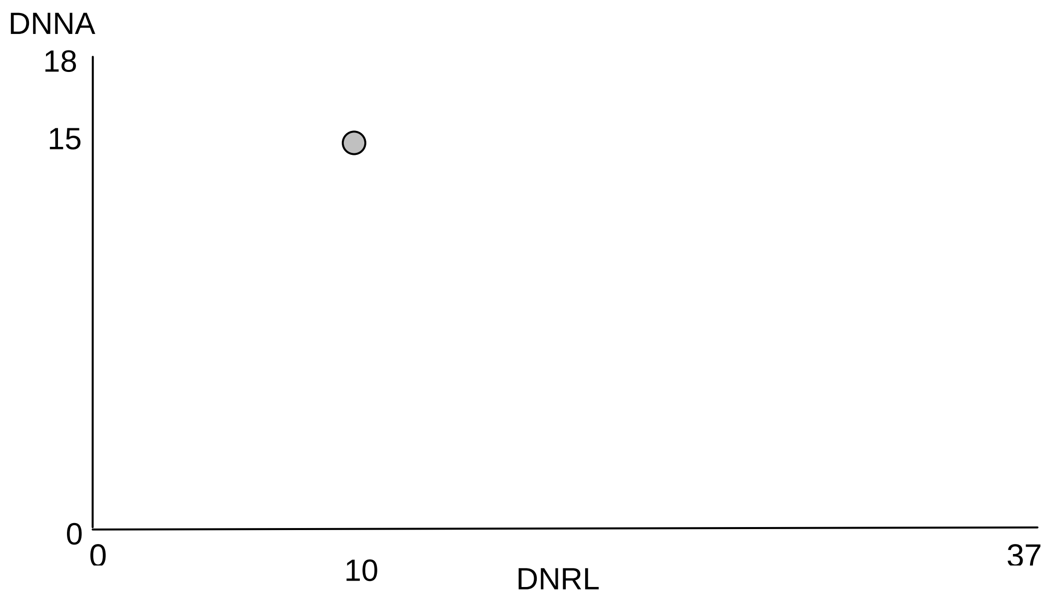

Here, a **gray color code** point symbol used to indicate that the density of this Y vs. X location is one (pixel). As other pairs of DN values are used to add points to this 2-Space plot, the blank (zero density) points begin to be occupied by one or more 2-Space points. Eventually, a pattern of high and low densities appear in the Y vs. X 2-Space plot.

A plot of all of the DN pairs in this 2-Space plot of Y (DNNA) vs. X (DNRL) values might look like the plot below:

Figure A19G. Many points in 2-Space: DNNA vs. DNRL.

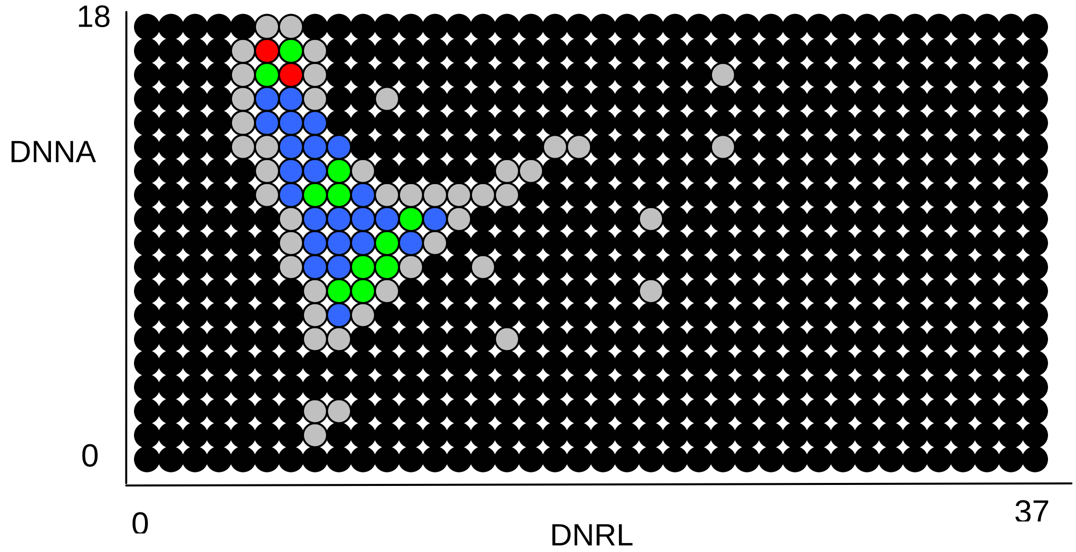

The **color code** here is the same as for the previous 1-Space plot.

A pattern emerges in this 2-Space plot of DNNA vs. DNRL. Most of the possible locations in this 2-Space plot are unoccupied by any points, i.e., have a density of **0**, as shown by **Black** symbols. Some locations have a point density of only **1** (**Gray**). Some have higher point densities or **2**, **3**, or **4** (Blue, Green, or Red).

Historical Note: Kauth and Thomas (1976) first defined the shape of this higher-density feature in a NA vs. RL 2-Space plot as the Tasseled Cap (TC) feature. The brim of the TC is along the **Green** points near the lower right edge of this data-cloud distribution. This is about where bare-soil pixels would be found in this 2-Space plot. The tip of the TC is at the top of the distribution where the highest-density locations are, i.e., the **Red** points. The tassel of the TC extends above and away from the tip (not visible in this coarse plot) and may even dip down into the triangular area of the TC itself.

The gap between the left-side of the TC and line where DNRL = 0 is caused by the steady reflectance of the atmosphere over the whole scene; no DNRL value can be lower than the DNRL associated with the reflectance of the atmosphere alone.

The width of the gap between the bottom of the TC distribution and the line where DNNA = 0 is small. Atmospheric reflectance is lower for the NA band than for the RL band.

The structure of the TC is better seen in an actual, detailed 2-Space plot of DNNA vs. DNRL from the Yuma, CO, QuickBird image of July 2, 2003:

Figure A19H. QuickBird Data in 2-Space: DNNA vs. DNRL.

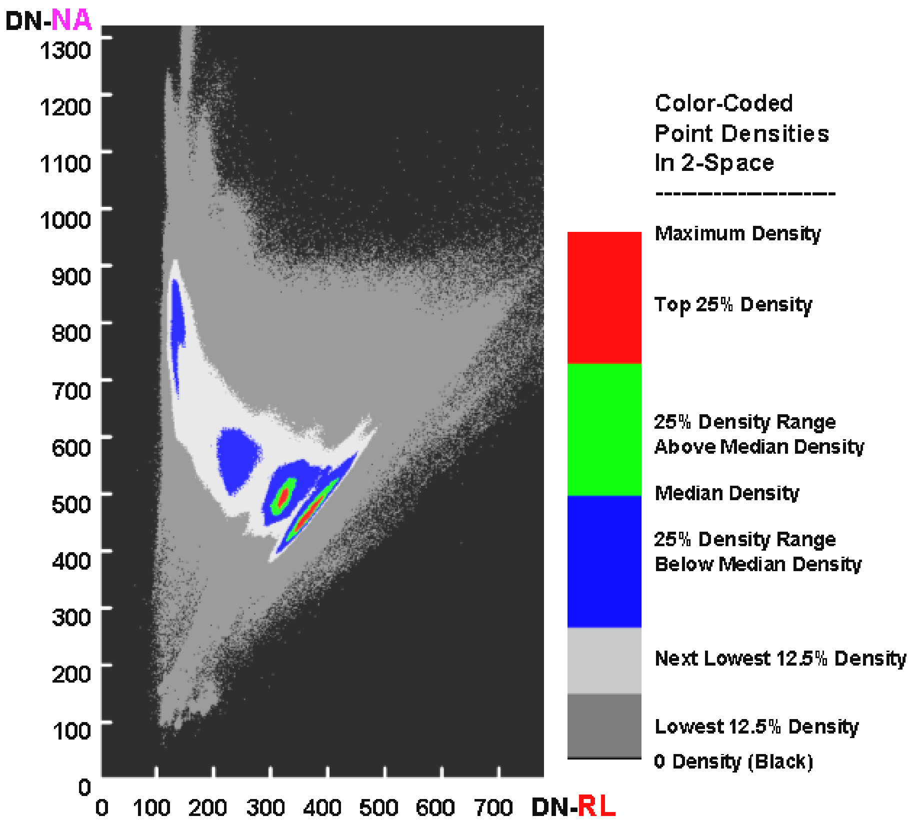

Here the lowest-density color, **Gray**, was divided into 2 sub-colors, **Dark Gray** & **Light Gray** (see the color code legend).

Most of this 2-Space has a data-cloud density of **0**. TNTmips has a Raster Correlation tool that shows a color-coded 2-Space data-cloud density plot based on 2 selected features, Y vs. X, e.g., NA vs. RL. It also shows each of the two related 1-Space plots as a pair of X-Y Line Histograms. One 1-Space Histogram plot is parallel to the X axis (assigned to RL in this case); the other 1-Space Histogram plot is parallel to the Y axis (assigned to NA in this case).

With standard TNTmips-provided colors for the relative density of the related 2-Space data cloud, this 2-Space plot looks is shown on the next page (same Yuma, CO, data set).

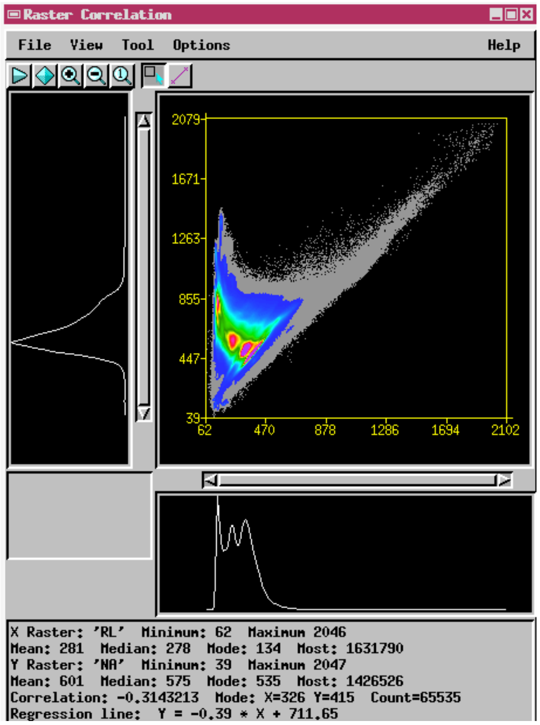

Figure A19I. QuickBird DNs in 2-Space: NA vs. RL with Standard Raster Correlation Color Lookup Table.

The TC shape to this data-cloud density 2-Space plot is clearly visible as the greenish to yellowish to reddish colors. Within the TC triangle are four clusters of high density points (red). The lower-right elongated red cluster is called the Line of Bare Soils. The red cluster above and to the right of it is associated with senesced vegetation pixels from a spring crop. The other two red-clusters are summer crops. The one with the highest NA value is maturing corn. Some wheat fields in the scene have very high NA values (around 1400). These are Tassels in the TC distribution.

The low-density (Gray) features extend to the upper right-hand corner of 2-Space. These are roof tops and road materials.

Low-density features extend below and to the left of the Line of Bare Soils. These are open water. Some pixels in this scene sit on the boundary between two materials, e.g., on the edges of water bodies. This materials mixture causes the affected pixels to occupy points in 2-Space that are between the locations of the several end-members of the mixture. Often, end members may consist of only two features, e.g., background soil mixed with foreground vegetation. In many cases, shadow is an additional end member (acts like it has a reflectance near zero in both bands). In other cases, the mixture involves three or more materials such as vegetation mixed with both a light and dark soil.

Vegetation Indices (VIs) represent a solution to the mixing problem for cases where the mixture involves one type of dominant foreground vegetation and two types of background soil: dark and bright soil, e.g., due to being wet and dry. This will be explored further in the *FAQ by Jack_E.pdf* tutorial related to the GRUVI.sml[6] script.

[6] **GRUVI** stands for **GR**and **U**nified **V**egetation **I**ndex. The GRUVI script contains control parameters that turn GRUVI output products into one of the classic VIs products into an optimized GRUVI product that deals best with the specific characteristics of a particular scene being analyzed.

The TC distribution can be easily recognized in a 2-Space plot for image data taken in an agricultural area. However, the TC distribution actually exists in a higher-dimensional 3-Space, 4-Space, etc. When more than two spectral bands are present in a MS data set, then each possible 2-Space plot represents of projection of the whole data cloud, which is in n-Space, in the view defined by the coordinate axis of each 2-Space pair.

3-Space

Consider how the DNs in three of the spectral bands of QuickBird MS plot out in a 3-dimensional Feature Space called 3-Space. In particular, examine the MS data cloud in the 3-Space associated with the DNs in the GL, RL, and NA rasters. Any view of a data cloud in 3-Space on a 2-D page (e.g., in this tutorial) must be a projection along a designated line of sight. Below is a perspective view of the 3-Space as seen along a line of sight that looks back toward the 3-Space origin defined by GL = 0, RL = 0, and NA = 0:

The 3-D data cloud is outlined in yellow. On each “wall” of the 3-Space is a shadow that outlines how the data cloud looks from the related perspective direction. There are three cardinal perspectives: NA vs. RL, NA vs. GL, and RL vs. GL. There are an infinite number of other perspectives; however, viewing the data cloud in these three cardinal 2-D perspectives leaves you with an impression of the 3-D structure of the data cloud in 3-Space.

Figure A19J. Oblique View of 3-Space.

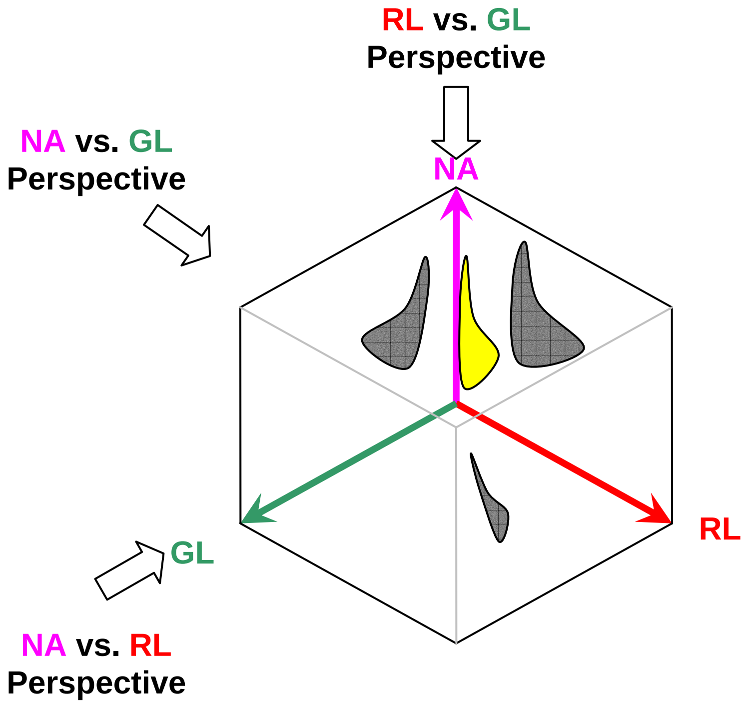

Figure A19K. Three Perspective Views of QuickBird DNs in 3-Space.

Below are the three perspective views of the actual data cloud related to the QuickBird MS scene over Yuma, CO, collected on July 2, 2003.

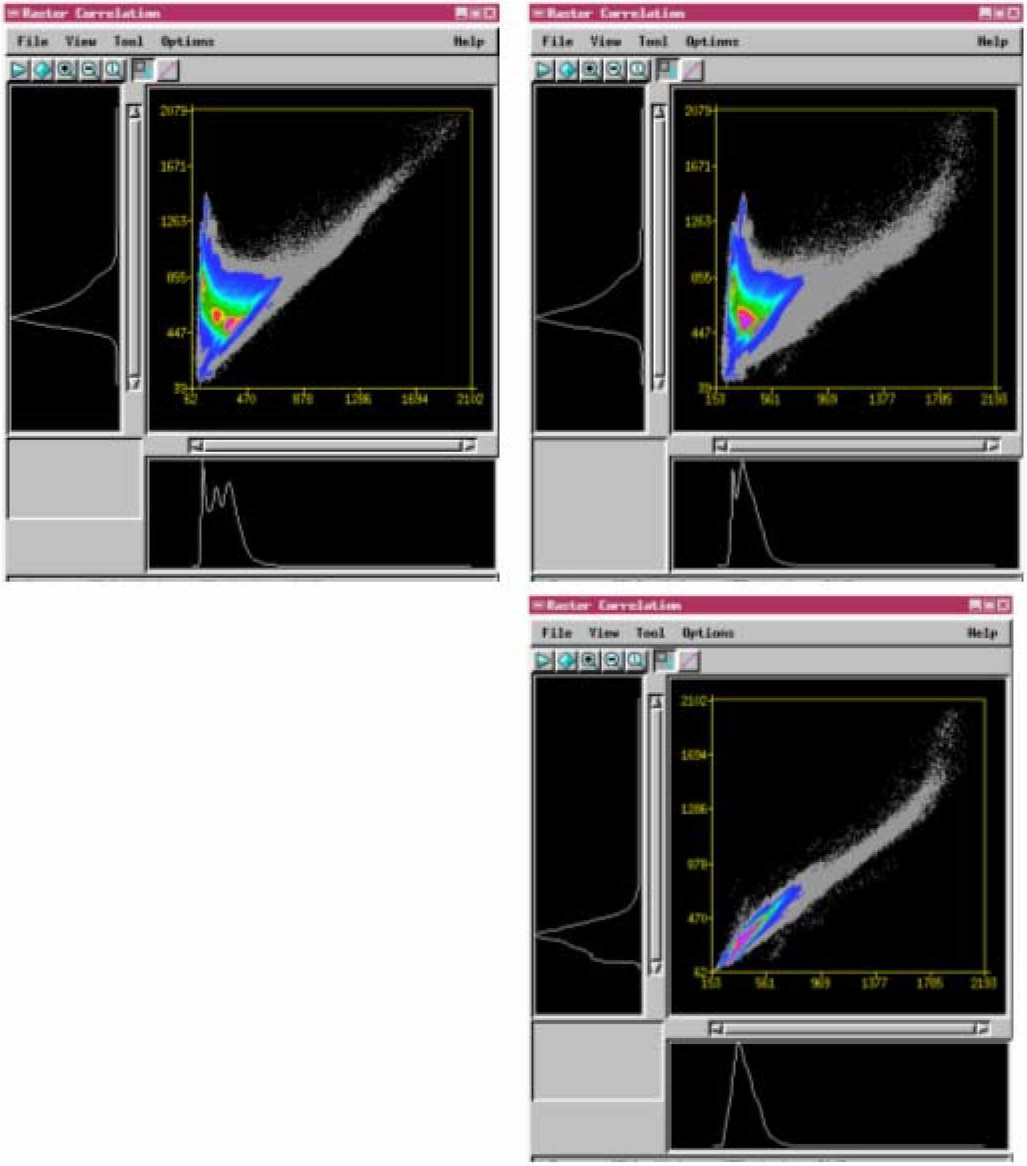

These figures here show 3 orthogonal perspective views of the Yuma, CO, QuickBird MS data cloud. The upper-left figure is DNNA vs. DNRL. The upper-right figure is DNNA vs. DNGL. The lower-right figure is DNRL vs. DNGL.

From these views, we get an impression that most of the data-cloud points are located on a 2-D plane, which is called the Tasseled Cap (TC) triangle. The DNRL vs. DNGL view looks pretty much directly across the edge of the

TC triangle. The other two views look more directly at the face of the TC triangle but at oblique angles to that face.

TASCAP.sml allows users to transform n-Space to produce a perfectly perpendicular view of the face of the TC triangle and a perfectly-aligned view across the edge of the TC triangle. The outputs from TASCAP.sml may be used by GRUVI.sml to reduce background noise. All of these scripts start with MS DN data that have been converted to Standardized Reflectance Factor Index (SRFI) values and that possibly have been corrected for terrain effects by TERCOR.sml. Key parameters from DIAG.sml are used by GRUVI.sml.

A20. What are Scale-Preserving Transformations of n-Space?

Spectral information extraction algorithms some times involve conversion of one MS data in n-Space to another set of MS data in a different transformed n-Space. If the coordinates of the source n-Space are calibrated, e.g., converted to SRFI values, then, it is desirable to preserve the SRFI scale in the new transformed n-Space. This is called a scale-preserving transformation.

Two basic kinds of transformations preserve scale in n-Space:

- Translation (T), which is a shifting of the coordinates to higher or lower values by adding a constant offset value to each SRFI value. The offset can be positive or negative.
- Rotation (R), which uses a matched set of sine and cosine functions, based on specified rotation angles, to rotate the coordinate axes without expansion, distortion, or contraction of the affected n-Space.

In 2-Space, the T algorithms are:

$$x2 = x1 + xoffset \qquad \text{(A20A)}$$
$$y2 = y1 + yoffset \qquad \text{(A20B)}$$

And the R algorithms are:

$$x3 = x2\ \cos(rang) - y2\ \sin(rang) \qquad \text{(A20C)}$$
$$y3 = x2\ \sin(rang) + y2\ \cos(rang) \qquad \text{(A20D)}$$

where **rang** is the rotation angle in degrees with a positive angle being in the clockwise direction.

The rotation angle, rang, might be small, e.g., to position the Line of Background Materials (LBM) related to bare soils at a place where y3 = x3 to prepare the data for the GRUVI.sml algorithm (see E). Or, rang, might be large, e.g., to position the LBM on the new x3 axis (where y3 = 0) to convert the data into “perpendicular” indicators of vegetation amount and soil brightness (called PVI and PBI, respectively).

T and R algorithms may be done in any sequence and any number of times without materially affecting the relative distances between two points in 2-Space nor the relative angles among three points in 2-Space. The primary goal for using TR algorithms is to move a key feature in 2-Space to a more ideal location in a new transformed 2-Space. As will be seen below, this sets up a new 2-Space to better correspond to the needs of an information-extraction algorithm, for example, a Vegetation Index (VI) algorithm.

TR algorithms may be applied to uncalibrated image DNs. However, it is better to convert image DNs to a calibrated metric, such as SRFI values, before doing a TR transformation to prepare the data for information extraction. The calibration process usually involves offsets and rescaling operations, not T and R *per se*. Spatially-dependent corrections may also be involved during calibration, e.g., terrain corrections (see TERCOR.sml and *FAQs_by_Jack_D.pdf*).

In *A19*, we examined a data cloud, as a 2-Space plot, from the Yuma, CO, QuickBird RL and NA data collected on July 2, 2003. Using the Line Equation and Point Report tools in the TNTmips Raster Correlation tool, we could determine specific values for rang, xoffset, and yoffset as related to the cluster of points associated bare-soil pixels on the LBM. This skill is addressed thoroughly in *FAQs_by_Jack E.pdf* (*E4*).

For the subject Yuma, CO, DNs, these parameters are as follows:

LBM (bare soil) slope = 1.2667
rang = -arctangent(slope) = -51.7106 degrees
xoffset = -94
yoffset = -119

Using these parameters, a TR transformation of the Yuma QB DNs for RL and NA produces in integer values for x3 and y3 that can be assigned to two new rasters, PBI and PVI. In this case, the DNs were shifted (translated) to a new origin (at x1 = 119 and y1 = 94) and then are rotated by -51.7106 degrees to align the LBM with the new x3 axis (where y3 = 0). The new y3 axis becomes a Perpendicular Vegetation Index (PVI). The new x3 axis becomes a Perpendicular Brightness Index (PBI).

PBI and PVI have the 2-Space plot characteristics shown on the next page. Also shown, on the next page, is the 2-Space plot of the related RL and NA data (same as in *A19*).

Figure 20A: NA vs. RL: QuickBird Image Data from Yuma CO, July 2, 2003.

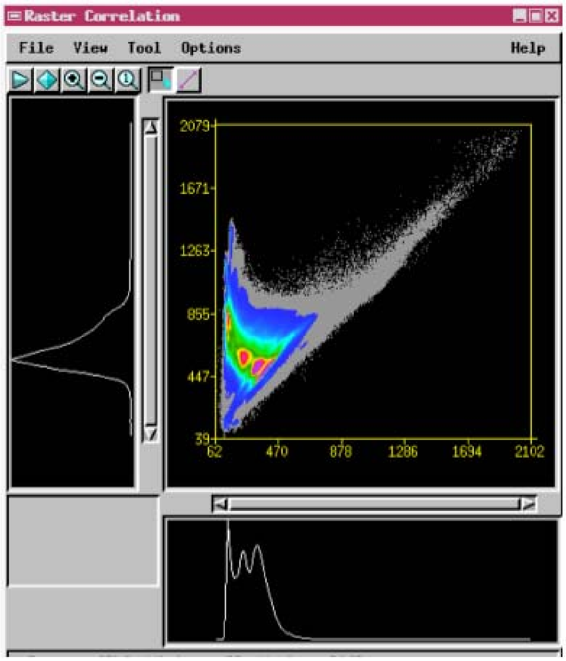

Figure 20B: PVI vs. PBI: T and R Transformed Data from Same Yuma Scene.

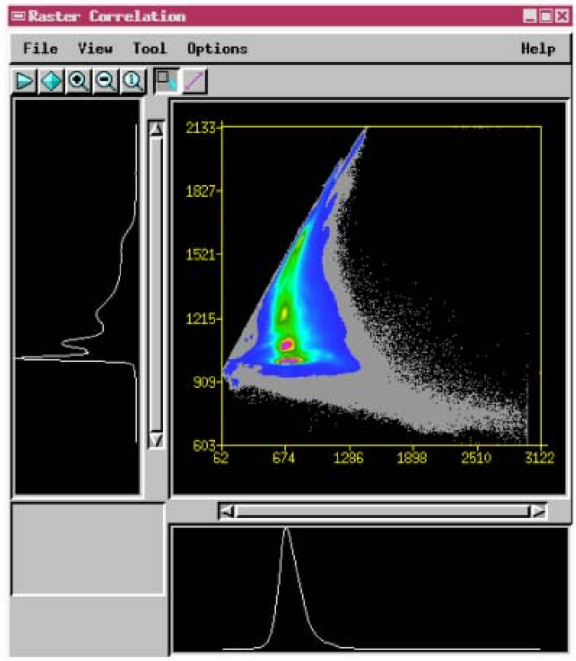

A counterclockwise rotation (negative rang value) of 2-Space axes causes the features in the 2-Space to appear to rotate in a clockwise direction.

The advantage of the new 2-Space data cloud in *Figure 20B* is that the bare-soil pixels are located on or near the horizontal line defined by PVI = 0. However, these particular PVI and PBI values are not optimal in that they are based on uncalibrated DN values from the original RL and NA rasters. As will be explained in detail in later tutorials and related SML scripts, it is better to convert DNs to a calibrated index, e.g., to SRFI values, *before* performing T and R operations that move certain features in SRFI 2-Space to new locations (like those in *Figure 20B*).

A21. How Do NDVI and SAVI Relate to TR Transformations?

The Normalized Difference Vegetation Index (NDVI, Rouse *et al.*, 1967) and Soil Adjusted Vegetation Index (SAVI, Huete, 1988) are defined in terms of Standardized Reflectance Factors (SRFs, in units of fractional reflectance) for NA and RL as follows:

NDVI = (SRFNA – SRFIRL) / (SRFNA + SRFRL) (A21A)

SAVI = (SRFNA – SRFRL)(1 + L) / (SRFNA + SRFRL + L) (A21B)

where L = 0.5, which is SAVI Soil Noise Factor. The possible range of values for NDVI and SAVI are from -1 to + 1; so, multiplicative scaling factors are often applied to each to produce raster values appropriate for output NDVI and SAVI rasters. Negative values are usually set equal to 0 or 1 an output NDVI or SAVI raster. This practice can lead to unreasonable consequences, especially when the algorithms are wrongly applied to uncalibrated image DNs.

NDVI was a strictly empirical algorithm. It has been widely adopted by the remote-sensing community. Unfortunately, the NDVI algorithm is wrongly applied to uncalibrated image DNs rather than to calibrated reflectance-factor data. SAVI was based on calibrated reflectance-factor data. The SAVI algorithm is better than the NDVI algorithm in that it quantifies the effects of background soils that have variable reflectance factors affecting both the NA and the RL bands. But, since NDVI came first, it was widely adopted.

Both NDVI and SAVI have a value of zero when SRFNA = SRFRL. So, if the Line of Background Materials for bare soil (LBM) were located *on* the line in 2-Space where SRFNA = SRFRL, the value of NDVI and SAVI for bare soils would be 0. Zero is an easy to understand value for a Vegetation Index of bare soil pixels. Unfortunately, Nature did not put the LBM for bare soils exactly on the line where SRFNA = SRFRL! According to Rondeaux *et al.*, (1996), the LBM for bare soil in NA vs. RL 2-Space is most likely to be defined by:

SRFNA = 0.0254 + 1.086 * SRFRL (A21C)

If 2-Space is transformed to make SRFINA3 = SRFIRL3 for pixels on the LBM for bare soil, NDVI and SAVI will both be equal to **0**. These and other Vegetation Indices, in general, will be discussed in greater depth in the tutorial related to GRUVI.sml.

Further discussions about these topics are provided in the tutorials related to the SML scripts for parameters such as SRFI, PBI, PVI, GRUVI, and GRUBI.

REFERENCES

Chander, G., and B. Markham, 2003: Revised Landsat 5 TM radiometric calibration procedures and post-calibration dynamic ranges. IEEE Trans. on Geoscience and Remote Sensing. 41 (11): pp. 2674-2677.

Chavez, P. S., Jr., 1996: Image-based atmospheric corrections revisited and improved. *Photogrammetric Engineering and Remote Sensing*, 62:1025-1036.

Crist, E. P. and R. C. Cicone, 1984: A Physically-Based Transformation of Thematic Mapper Data--The TM Tasseled Cap," in *IEEE Transactions on Geoscience and Remote Sensing*, Vol. 22, No. 3, May 1984, pp. 256-263

Clevers, J.G.P.W., 1988: The derivation of a simplified reflectance model for the estimation of leaf area index. *Remote Sensing of Environment*, 25, pp. 53-69.

Huete, A., 1988: A Soil-Adjusted Vegetation Index (SAVI). Remote Sensing of Environment, 25, pp. 295-309.

Kauth, and Thomas, 1976: The Tasseled Cap -- A Graphic Description of the Spectral-Temporal Development of Agricultural Crops as Seen by LANDSAT. *Proceedings of the Symposium on Machine Processing of Remotely Sensed Data*, Purdue University of West Lafayette, Indiana, 1976, pp. 4B-41 to 4B-51.

Krause, K., 2004: *Radiance Conversion of QuickBird Data.* Technical Note, www.digitalglobe.com., 4 pp.

Lillesand, T. M., R. W. Kiefer, and J. W. Chipman, 2004: *Remote Sensing and Image Interpretation*, 5th Ed., John Wiley & Sons, Inc., Hoboken, NJ, 763 pp.

Pasachoff, J. M., and M. L. Kutner, 1978: *University Astronomy.* W. B. Sanders Co., Philadelphia, 763 pp.

Rondeaux, G., M. Steven, and F. Baret, 1996: Optimization of soil-adjusted vegetation indices. *Remote Sensing of Environment*, 55:95-107.

Rouse, J. W., R. H. Haas, J. A. Schell, and D. W. Deering, 1973: Monitoring vegetation systems in the Great Plains with ERTS, Third ERTS Symposium, NASA SP-351_, vol. 1, pp.309-317.

Smith, R. B., 2001: *Introduction to Remote Sensing of Environment (RSE).* MicroImages, Inc., 11th Floor, Sharp Tower, 206 South 13th Street, Lincoln, NE 68508-2010 USA, www.microimages.com.

Smith, R. B., 2003: *Building Dialogues in SML.* MicroImages, Inc., 11th Floor, Sharp Tower, 206 South 13th Street, Lincoln, NE 68508-2010 USA, www.microimages.com.

Smith, R. B., and K. Ghormley, 2003: *Writing Scripts with SML.* MicroImages, Inc., 11th Floor, Sharp Tower, 206 South 13th Street, Lincoln, NE 68508-2010 USA, www.microimages.com.

Weast, R. C., ed., 1985: *CRC Handbook of Chemistry and Physics*. 66th Ed., CRC Press, Inc., Boca Raton, FL